

 Very Important Paper


Exploring the Translational Gap of a Novel Class of *Escherichia coli* IspE Inhibitors

Henni-Karoliina Ropponen⁺,^[a, b, e] Eleonora Diamanti⁺,^[a] Sandra Johannsen,^[a, b] Boris Illarionov,^[c] Rawia Hamid,^[a, b] Miriam Jaki,^[a, b, f] Peter Sass,^[d] Markus Fischer,^[c] Jörg Haupenthal,^[a] and Anna K. Hirsch^{*[a, b]}

Discovery of novel antibiotics needs multidisciplinary approaches to gain target enzyme and bacterial activities while aiming for selectivity over mammalian cells. Here, we report a multiparameter optimisation of a fragment-like hit that was identified through a structure-based virtual-screening campaign on *Escherichia coli* IspE crystal structure. Subsequent medicinal-chemistry design resulted in a novel class of *E. coli* IspE

inhibitors, exhibiting activity also against the more pathogenic bacteria *Pseudomonas aeruginosa* and *Acinetobacter baumannii*. While cytotoxicity remains a challenge for the series, it provides new insights on the molecular properties for balancing enzymatic target and bacterial activities simultaneously as well as new starting points for the development of IspE inhibitors with a predicted new mode of action.

Introduction

The bottleneck in discovering new antibiotics arises from the very first steps of research due to the difficulty to find novel compounds and targets that do not exhibit cross-resistance, as defined by the innovative criteria set by the World Health Organisation.^[1] Over the past years, several rules have been developed to speed up the discovery of ideal antibiotic candidates, particularly against Gram-negative pathogens.^[2] In a review, A. L. Parkes raised the most fundamental question in antibiotic research, “what can we design for?”^[3] There are contradicting opinions on which of the rules are actually of importance. Successful antibiotic drug design should be guided by the recently introduced concept of bacterial bioavailability that accounts for a holistic balance of bacterial uptake, distribution, metabolic and efflux pathways.^[2] The outer membrane of Gram-negative bacteria represents an extra hurdle for compounds to enter the cells in comparison to their Gram-positive counterparts. Essentially, compounds can be actively transported through membrane porins and pumps or pass passively through the phospholipid layers.^[4] In 2017, Richter et al. reported the so-called eNTRY rules aiming for a good accumulation into Gram-negative *Escherichia coli* bacteria.

The eNTRY rules state that a well-accumulating compound needs an ionisable amine (N), preferably a primary amine, low globularity (≤ 0.25) (T=three-dimensionality) and rotatable bonds (≤ 5) (R=rigidity). Based on the eNTRY rules, ionisable amines provide better accumulation due to a key electrostatic interaction with the outer membrane porin F (OmpF).^[5] Although this LC-MS-based accumulation study focused only on Gram-negative *E. coli*, the follow-up studies have also suggested a broader applicability of the rules for other Gram-negative bacteria, namely *Acinetobacter baumannii* and *Klebsiella pneumoniae*.^[6] The activity against the less permeable *Pseudomonas aeruginosa*, however, is often lacking and we questioned the overall applicability of the rules in an amino acid modified series.^[2, 7] Good accumulation and permeability into the cytoplasm are important in order to achieve good inhibition of intracellular enzymes. In this study, we focus on evaluating the cytoplasmic 2-C-methyl-D-erythritol 4-phosphate (MEP) pathway that is vital for the biosynthesis of universal isoprenoid precursors.^[8] Since the same isoprenoid precursors are synthesised via the distinct mevalonate pathway in humans, the bacterial MEP pathway is a rich source of attractive anti-infective drug targets.^[9] Clinical proof of concept and validation of the enzymes of the MEP pathway was demonstrated by fosmidomycin, an inhibitor of

[a] Dr. H.-K. Ropponen,⁺ Dr. E. Diamanti,⁺ Dr. S. Johannsen, R. Hamid, M. Jaki, Dr. J. Haupenthal, Prof. A. K. H. Hirsch
Drug Discovery and Optimization
Helmholtz Institute for Pharmaceutical Research Saarland (HIPS)
Helmholtz Centre for Infection Research (HZI)
Campus Building E8.1, 66123 Saarbrücken (Germany)
E-mail: anna.hirsch@helmholtz-hips.de

[b] Dr. H.-K. Ropponen,⁺ Dr. S. Johannsen, R. Hamid, M. Jaki, Prof. A. K. H. Hirsch
Saarland University, Department of Pharmacy
Campus Building E8.1, 66123 Saarbrücken (Germany)

[c] Dr. B. Illarionov, Prof. M. Fischer
Hamburg School of Food Science, Institute of Food Chemistry
Grindelallee 117, 20146 Hamburg (Germany)

[d] Dr. P. Sass
Interfaculty Institute of Microbiology and Infection Medicine
Universität Tübingen <postCode/ 72076 < Tübingen (Germany)

[e] Dr. H.-K. Ropponen⁺
Current address: AMR Action Fund GP GmbH
Messeplatz 10, 4058 Basel (Switzerland)

[f] M. Jaki
Current address: University of Freiburg, Institute of Pharmaceutical Sciences
Department of Pharmaceutics, Sonnenstraße 5, 79104 Freiburg (Germany)

[*] These authors contributed equally to this work.

 Supporting information for this article is available on the WWW under <https://doi.org/10.1002/cmdc.202300346>

 © 2023 The Authors. ChemMedChem published by Wiley-VCH GmbH. This is an open access article under the terms of the Creative Commons Attribution License, which permits use, distribution and reproduction in any medium, provided the original work is properly cited.

1-deoxy-D-xylulose-5-phosphate reductoisomerase (DXR or IspC), that is in clinical trials to treat malaria.^[10] It also inhibits multidrug-resistant bacterial strains, such as *P.aeruginosa*.^[11] However, to the authors' knowledge, comparably advanced success stories with other compounds targeting the bacterial MEP pathway have not yet been reported. In the search for novel inhibitors of the MEP pathway, we focused on the fourth enzyme IspE that phosphorylates the natural substrate 4-diphosphocytidyl-2-C-methyl-D-erythritol (CDP-ME) to afford 4-diphosphocytidyl-2-C-methyl-D-erythritol 2-phosphate (CDP-MEP) in the presence of ATP. Most of the previously reported IspE inhibitors against Gram-negative *E. coli* have low-micromolar enzyme activity but report no activity in whole-cell assays.^[2,4] Yet, IspE was examined to be a moderately druggable target in *E. coli*.^[12] To address this translational gap, we embarked on an *in silico* virtual screening (VS) of the commercially available SPECS library of 106,801 compounds using the crystal structure of *EclspE* (PDB 1OJ4) and applying the eNTRY rules in the filtering process to obtain hits with a high *E. coli* accumulation.^[13]

Results and Discussion

We selected the catalytic, ATP-binding pockets of *EclspE* as the binding pocket for the VS based on the druggability assessment using DogSiteScorer (details are reported in the Supporting Information (SI) Section 1.1), and used BioSolveIT software (LeadIT for docking and SeeSAR for scoring) to perform the VS (Figure S1).^[14] Previously, we published other *EclspE* inhibitors addressing the same catalytic site and other VS campaigns have also been conducted using *EclspE* (PDB 1OJ4).^[15] Most of these inhibitors, however, lack the needed antibacterial cell activity and to the best of our knowledge, they have not been further developed. Thus, by implementing the eNTRY rules into the filtering process of the VS library, we aimed to find a hit with both cellular activity against *E. coli* and inhibitory activity against the enzyme *EclspE*. The selection of VS hits included a mixture of compounds with different degrees of ionisation of the ionisable amine (Table S1). In addition, we also selected a few compounds simply with the highest estimated HYDE-binding affinities and a few compounds based on a novel antibacterial scoring profile developed by Optibrium.^[16] The original research paper on the eNTRY rules pinpoints that most of the commercially available libraries do not contain enough primary amines, concluding this might be one of the reasons for unsuccessful screening campaigns in the search for novel antibacterial candidates.^[5a] Overall, the particular SPECS library we used comprised 70 primary amines and we decided to test twelve additional primary amines that had not passed the VS filters.

Hit selection

Disappointingly, out of the 24 compounds (1–24) we purchased after the applied VS filters, none displayed *EclspE* inhibition in the primary screening and even those showing slight *EclspE* inhibition also inhibited the auxiliary enzymes, pyruvate kinase and lactate dehydrogenase (PK/LDH), in the coupled enzyme assay (Tables S2–6).^[17]

Furthermore, we tested twelve additional primary amines (25–36, Table S7) that had not passed the VS filters. They were also tested against *E. coli* and out of them, three compounds showed moderate inhibition (e.g., the tricyclic scaffold **27** ($50 \pm 8\%$ inhibition of *E. coli* K12 at 100 μM and $81 \pm 0\%$ inhibition of *E. coli* ΔtolC), the thiazole **33** ($76 \pm 16\%$ inhibition of *E. coli* K12 at 100 μM and minimum inhibitory concentration (MIC) = $98 \pm 11 \mu\text{M}$ of *E. coli* ΔtolC) and another tricyclic compound **36** ($57 \pm 4\%$ inhibition of *E. coli* K12 at 100 μM and $79 \pm 1\%$ inhibition of *E. coli* ΔtolC) (Table S7). These twelve compounds were not further exploited in our laboratory, but they may provide an interesting starting point for further optimisation.

Thereby, we made a top-three hit selection (Table S8) based on the multiparameter evaluation considering antibacterial activity, *in vitro* and/or *in silico* *EclspE* engagement and cytotoxicity. The compounds in the top-three selection are structurally different and include primary, secondary and tertiary amines (**2**, **15** and **14**, respectively). They all have a promising antibacterial-activity profile, inhibiting *E. coli* K12 and ΔtolC , measured as percentage inhibition at the highest solubility, where no MIC could be measured. We also tested them against the more pathogenic Gram-negative strains, *P.aeruginosa* PA14 and *A. baumannii*, as well as against Gram-positive *Staphylococcus aureus* and *Bacillus subtilis* (Table S8). Importantly, the MEP pathway is mainly present in Gram-negative bacteria and only exists in some selected Gram-positive bacteria, including *B. subtilis*.^[18] We therefore included the Gram-positive strains *S. aureus* and *B. subtilis* as a negative and positive control, respectively, providing a first indication of target engagement with the enzyme IspE and we validated the interference of **15** with the MEP pathway in live *B. subtilis* cells via comparative phenotype profiling (Figure S2). Both **2** and **15** showed poorer activities against *S. aureus* and *B. subtilis* than *E. coli* K12, supporting the expected activity profile for MEP inhibitors although acknowledging the non-selective nature of our early hit compounds. Later, we used biophysical assays to examine binding to *EclspE* and enzyme-activity assays revealed the secondary amine derivative **15** and another compound from the VS **19** to inhibit *EclspE* (Table S5). However, we have not followed up on them to date due to their weaker antibacterial profiles.

Hit validation

Overall, the primary amine derivative **2** possessed the most promising starting point for further optimisation due to its fragment-likeness (MW = 261.7 g/mol). After resynthesis (Scheme S1) and validation of the hit compound, we evaluated its binding affinity using the thermal shift assay (TSA) and microscale thermophoresis (MST), showing a shift in melting point ($T_m = 50.42 \pm 0.09 (-1.1)^\circ\text{C}$, Table S13) and weak binding to *EclspE* ($K_D \sim 700 \mu\text{M}$, Table S14). We also confirmed its binding with *EclspE* using saturation-transfer difference (STD)-NMR spectroscopy (Spectrum S1). Based on the lack of *in vitro* *EclspE* activity, it was clear that IspE is not the only target. Nevertheless, it is still unclear how strong the MEP pathway target needs to be bound for cellular inhibition. Therefore, due to its fragment-likeness with the opportunity to explore and expand its chemical structure, we

decided to proceed with the primary amine hit **2** to evaluate its potential to increase the affinity for *EclspE* and in parallel, focusing on understanding the structure–permeation relationship for antibacterial activity through subtle handle modifications while simultaneously addressing the cytotoxicity flag (**2**, HepG2 IC_{50} = $21 \pm 1 \mu\text{M}$, Table 1).

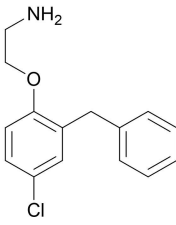
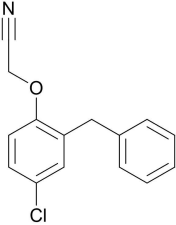
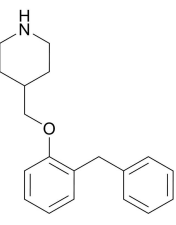
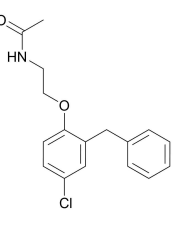
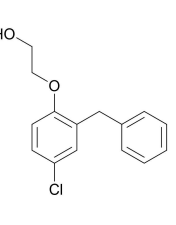
The resynthesis of **2** began from the corresponding phenolic derivative followed by introduction of the handle via an S_N2 reaction (Scheme S1). In order to evaluate the need for the primary amine, we tested all the synthetic derivatives, the phenolic core **37** and the nitrile-handle **38** derivatives, and confirmed that the primary amine indeed boosted the activity against the wild-type *E. coli* K12 (Table 1 and Table S9). These slight modifications in the handle, hereafter called the ‘activity handle’, further encouraged us to move on with the series aiming to evaluate the molecular causes leading to differential

antibacterial activities. In addition, a similar ethanolamine handle was used for arylomycin derivative G0775 to increase antibacterial activity against a panel of Gram-negative bacteria, also against *P. aeruginosa*.^[6e]

Multiparameter optimisation: evaluation of various activity handles

As the next step, we investigated several commercially available (**39–56**) close derivatives of the hit **2**, mainly focusing on different modifications of the activity handle. These compounds were tested against multiple *E. coli* mutant strains as well as the target enzyme *EclspE* (a comprehensive list is given in Table S10). None of the activity-handle modifications exhibited clear *EclspE* activity, however, thioether **43** showed slight

Table 1. Comparison of the different activity handles.

					
	2	38	46	47	49
Minimum Inhibitory Concentration (MIC) or Percentage Inhibition at 100 μM					
<i>Escherichia coli</i> K12	$99 \pm 2 \mu\text{M}$	$13 \pm 2\%$	$13 \pm 11\%$	n.i.	$27 \pm 3\%$
<i>Escherichia coli</i> $\Delta\text{tolC}^{[a]}$	$97 \pm 4 \mu\text{M}$	$38 \pm 1 \mu\text{M}$	$85 \pm 8\%$	$88 \pm 11 \mu\text{M}$	$50 \pm 0 \mu\text{M}$
<i>Escherichia coli</i> $\Delta\text{acrB}^{[a]}$	$95 \pm 0 \mu\text{M}$	$54 \pm 5\%$	$108 \pm 4 \mu\text{M}$	$30 \pm 12\%^{[g]}$	$103 \pm 3 \mu\text{M}$
<i>Escherichia coli</i> D22 ^[c]	$105 \pm 7 \mu\text{M}$	$35 \pm 5 \mu\text{M}$	$67 \pm 4\%$	$34 \pm 6\%^{[g]}$	$22 \pm 4\%$
<i>Escherichia coli</i> $\text{Omp8}^{[b]}$	$87 \pm 7\%$	n.d.	$58 \pm 5\%$	n.i. ^[g]	$104 \pm 2 \mu\text{M}$
<i>Pseudomonas aeruginosa</i> PA 14	$52 \pm 10\%$	n.i.	$43 \pm 9\%$	n.i. ^[g]	n.i.
<i>Pseudomonas aeruginosa</i> $\Delta\text{mexB}^{[a]}$	$33 \pm 9\%$	n.d.	$35 \pm 21\%$	n.i. ^[g]	n.d.
<i>Pseudomonas aeruginosa</i> $\Delta\text{mexA}^{[a]}$	$49 \pm 25\%$	n.d.	$43 \pm 10\%$	n.i. ^[g]	n.d.
<i>Pseudomonas aeruginosa</i> $\Delta\text{oprF}^{[b]}$	$59 \pm 27\%$	n.d.	$48 \pm 8\%$	$20 \pm 10\%^{[g]}$	n.d.
<i>Pseudomonas aeruginosa</i> $\Delta\text{omph}^{[a]}$	$48 \pm 5\%$	n.d.	$31 \pm 16\%$	n.i. ^[g]	n.d.
<i>Acinetobacter baumannii</i>	$100 \pm 0 \mu\text{M}$	n.i. ^[g]	$14 \pm 6\%$	n.i. ^[g]	n.i. ^[g]
<i>Staphylococcus aureus</i>	$47 \pm 8\%$	n.i. ^[g]	$20 \pm 10\%$	$22 \pm 6\%$	$32 \pm 21\%$
Cytotoxicity Inhibitory Concentration (IC_{50}) or Percentage Inhibition at 100 μM					
HepG2	$20 \pm 1 \mu\text{M}$	$80 \pm 3\%$	$21 \pm 4 \mu\text{M}$	$47 \pm 4\%$	$69 \pm 20\%$
Calculated properties					
$\text{clogD}^{[d]}$	1.6	5.2	2.0	4.1	4.3
Most basic $\text{pK}_a^{[e]}$	9.1	N/A	10.1	N/A	N/A
Amphiphilic moment ^[f]	7.3	6.5	5.2	5.0	5.4
[a] Efflux pump mutant. [b] Porin mutant. [c] Strain with defective LPS layer. [d] Calculated with StarDrop 7.0.1 at pH 7.4. [e] Calculated with StarDrop 7.0.1. [f] Calculated with MOE 2020.09 for the energy-minimised molecule. [g] Experiment performed at 50 μM . n.d.: not determined; n.i.: no inhibition, if inhibition < 10%; N/A: not applicable.					

inhibition ($EclspE$ IC_{50} = 447 μ M, from a single measurement), just as its close derivative **48** bearing the hydroxyl group in ortho-position ($EclspE$ IC_{50} = 356 \pm 46 μ M), and a slight decrease in the melting point (T_m = 51.10 \pm 0.08 (–0.4) $^{\circ}$ C, Table S13). Given that the sulfoxide derivative **44** showed no activity and also due to the fact that thioethers may oxidise to the sulfoxide in cellulose, we decided not to pursue in this direction.

We also screened some of the compounds featuring modifications in the activity handle, including hit **2** against different *E. coli* and *P. aeruginosa* mutants. In detail, e.g. the efflux pump mutants *E. coli* Δ acrB and *P. aeruginosa* Δ mexA were used to identify potential efflux issues, *E. coli* D22 has a defective lipopolysaccharide (LPS) layer that usually (in wild type strains) forms a dense protective hydrophilic barrier against entry of drugs, and *E. coli* Omp8 and *P. aeruginosa* Δ oprF possess mutated porins (Table 1). The nitrile-handle **38**, the amide **47** and hydroxyl **49** could further support the hypothesis that a primary amine is necessary, as all the other derivatives without an ionisable amine proved to be inactive against the *E. coli* K12 wild-type. Most of them only showed inhibition of *E. coli* Δ tolC growth, suggesting efflux issues may account for the lack of activity against *E. coli* K12. In addition, in case of **38**, **46** and **47**, the activities slightly increased against the LPS mutated *E. coli* D22, proposing the overall core scaffold also to form key interactions with the LPS layer. Nevertheless, we could demonstrate that the activity against the *E. coli* porin-knockdown mutant omp8, (BL21(DE3)omp8), lacking the major *E. coli* OmpF, OmpA and OmpC porins, with **2** suffered a 10% decrease in activity (%-inh. = 87 \pm 7% at 100 μ M), suggesting that **2** finds an alternative uptake mechanism despite the primary amine being present.^[19] Interestingly, the amide derivative **47** showed no inhibition against *E. coli* Omp8, unexpectedly hinting it relies more on porin uptake than the corresponding amine **2** in disagreement with the eNTRY rules (Table 1).

Next, we evaluated **58** (Scheme S1, Table S9) with a central diaryl ether linker and an aniline-linked activity handle, which lacked cellular activity despite the primary and secondary amine. However, its toxicity was lower than for **2**, (HepG2%-inh. = 48 \pm 7% at 100 μ M vs IC_{50} = 21 \pm 1 μ M), respectively. Removing the amines also helped with cytotoxicity (compounds **38** and **49**), but as previously mentioned also reduced their activity.

Given that some of the derivatives investigated showed some antibacterial activity against *E. coli* strains, we tested the best activity handle modifications against the more pathogenic bacteria *A. baumannii* and *P. aeruginosa* (Tables S9 and S10). Interestingly, the piperidine handle **46** showed slightly better % inhibition against *P. aeruginosa* wild-type PA 14 (%-inh. = 43 \pm 9 at 100 μ M) than *E. coli* wild-type K12 (%-inh. = 13 \pm 11 at 100 μ M), despite the lack of a chlorine atom in 4-position, lowering the amphiphilic moment. The general trend is that most of the compounds active against *E. coli* lose potency when moving to the more pathogenic bacteria. Only compound **2** showed some inhibition of *A. baumannii* (MIC = 100 \pm 0 μ M), indicating that the amino group plays a role for the activity. We also had the capability to test the latter two and the amide-handle derivative **47** as a negative control against other *Pseudomonas* mutant strains to evaluate the

potential efflux or permeability issues with outer-membrane porin mutants Δ oprF and Δ ompH, and efflux-pump mutants Δ mexB and Δ mexA.^[20] Surprisingly, we did not observe such striking activity differences as we had seen for the *E. coli* mutants, mainly with Δ tolC (Table 1). This could, however, suggest that there are other molecular properties governing the uptake and efflux ratios in *P. aeruginosa*, as supported by J. Ude et al., concluding that porin-independent permeation may play a bigger role in *P. aeruginosa* and yet, carboxylates favour permeation via porins.^[21]

Multiparameter optimisation: modifications of the amphiphilic moment

Next, we focused on altering the amphiphilic moment, as also described in the original eNTRY rules on our fragment hit **2**.^[5a] The amphiphilic moment is the distribution of or distance between the hydrophilic and hydrophobic parts of a compound. In the hit structure **2**, there is a high amphiphilic moment between the chlorine and the free amine (vsurf_A = 7.3). In simplicity, one can consider charge necessary to get through the outer membrane porins favourably and lipophilicity for passive uptake through the lipophilic polysaccharide bilayers either in the outer or the inner membrane, as earlier hinted by H. Nikaido et al.^[22] Therefore, to modify the amphiphilic moment, we synthesised a so-called halogen series (Table 2, Scheme S2), where the chlorine in 4-position was substituted by different halogens. The calculated amphiphilic moment increased when going down the halogen row in the periodic table. The intermediates from the synthesis have also been tested but were all poorer in inhibiting *E. coli* K12, re-emphasising the need for the primary amine (**59–67**, Tables S9 and S10).

We confirmed that the increased amphiphilic moment clearly boosted the activity when moving down the periodic table for all tested strains (Table 2). The iodine derivative led to a two-fold decreased MIC value against *E. coli* K12 and increased activity against *A. baumannii* and *P. aeruginosa*, but failed to improve the cytotoxicity profile.

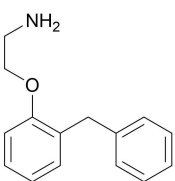
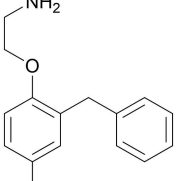
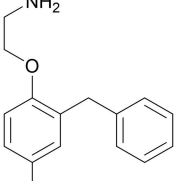
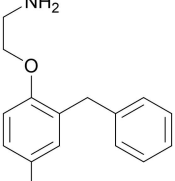
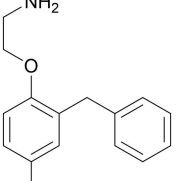
Multiparameter optimisation: introduction of dichloro substituents

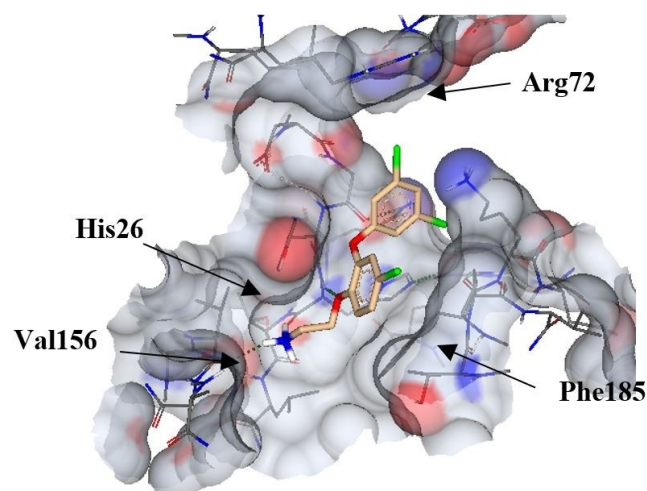
During the VS, some binding poses were observed to interact with Arg72 from the other monomer. In particular, this was seen with **15** ($EclspE$ = 253 \pm 24 μ M) bearing a dichloro motif. Therefore, with the aim to further explore this part of the binding pocket, we designed the dichloro-derivative **67** (Scheme S3) of the initial hit using the structure of $EclspE$ (PDB 1OJ4) (Figure 1, Table S11).

This dichloro motif was introduced on the right-hand side phenyl ring and for the first time, the series showed $EclspE$ inhibitory activity (IC_{50} = 159 \pm 4 μ M) with an increased binding affinity determined by MST (K_D ~60 μ M, Table S14). STD-NMR studies further confirmed the binding with $EclspE$ (Spectrum S2).

Based on the docking pose, the interaction of this dichloro-motif could disturb the dimerization of $EclspE$ by interacting

Table 2. Summary of the biological results for the halogen series to investigate the influence of the amphiphilic moment on the antibacterial activity.

					
	39	59	2	60	61
Minimum Inhibitory Concentration (MIC) or Percentage Inhibition at 100 μM					
<i>Escherichia coli</i> K12	31 \pm 5 %	38 \pm 2 %	99 \pm 2 μM	90 \pm 0 μM	53 \pm 4 μM
<i>Escherichia coli</i> $\Delta\text{tolC}^{\text{[a]}}$	41 \pm 0 %	48 \pm 6 %	97 \pm 4 μM	93 \pm 4 μM	88 \pm 4 μM
<i>Escherichia coli</i> $\Delta\text{acrB}^{\text{[a]}}$	42 \pm 1 %	44 \pm 11 %	95 \pm 0 μM	94 \pm 0 μM	84 \pm 5 μM
<i>Escherichia coli</i> $\text{Omp8}^{\text{[b]}}$	n.i.	n.i.	87 \pm 7 %	94 \pm 1 μM	75 \pm 10 μM
<i>Pseudomonas aeruginosa</i>	n.i.	11 \pm 1 %	52 \pm 10 %	70 \pm 3 %	52 \pm 6 %
<i>Acinetobacter baumannii</i>	22 \pm 1 %	11 \pm 1 %	100 \pm 0 μM	n.d.	95 \pm 0 μM
<i>Staphylococcus aureus</i>	11 \pm 7 %	n.i.	47 \pm 8 %	79 % ^[f]	86 \pm 8 %
Cytotoxicity Inhibitory Concentration (IC_{50}) or Percentage Inhibition at 100 μM					
HepG2	88 \pm 5 %	58 \pm 10 μM	21 \pm 1 μM	98 \pm 1 %	17 \pm 1 μM
Calculated properties					
clogD ^[c]	0.9	1.1	1.6	1.3	1.3
Most basic $\text{pK}_a^{\text{[d]}}$	9.3	9.3	9.1	9.1	9.1
Amphiphilic moment ^[e]	5.3	6.8	7.3	7.3	7.8
[a] Efflux pump mutant. [b] Porin mutant. [c] Calculated with StarDrop 7.0.1 at pH 7.4. [d] Calculated with StarDrop 7.0.1. [e] Calculated with MOE 2020.09 for the energy-minimized molecule. [f] Experiment performed at 25 μM . Value of a single measurement. n.d.: not determined; n.i.: no inhibition, if inhibition < 10%.					

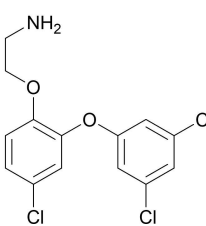
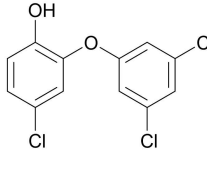
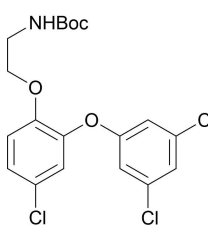
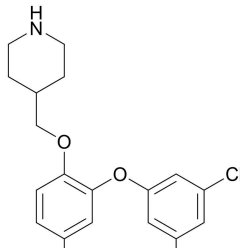
**Figure 1.** Binding site with **67** showing the possible interaction with the Arg72 from the other monomer in its predicted docking pose. Molecular modelling was done in SeeSAR 12.1 and the figure was created in StarDrop 7.0.1.^[14d]

with the residue Arg72 from the other monomer, potentially destabilising the enzyme, which could lead to a decreased melting point in a TSA. To the authors' knowledge, such a mode of action against *EclspE* has not been explored to date.

The dichloro-derivative **67** was also tested in TSA, where we indeed observed a decreased melting point ($\Delta T_m = -1.9^\circ\text{C}$, Table S13) in comparison to the native *EclspE* ($T_m = 51.5 \pm 0.14^\circ\text{C}$), being in the previously reported range.^[23] In comparison, the natural substrate CDP-ME shows an increased melting point ($\Delta T_m = +0.8^\circ\text{C}$). This was the first indication supporting the binding of **67** in the hydrophobic pocket, possibly disturbing the dimerisation, although it is not yet fully confirmed, whether the *EclspE* enzyme really exists as a dimer in solution.^[23] We tested all synthetic derivatives of the dichloro-series against *EclspE* and confirmed that the free amine **67** selectively inhibits *EclspE*, whereas the phenol derivative **68** also inhibits the auxiliary enzymes PK/LDH (Table S11). This was a key information for our further optimisation of the series.

As we had seen changes in activity between *E. coli* and *P. aeruginosa* with different activity handles (primary amine **2** vs piperidine **46**), we synthesised the dichloro-derivative using a piperidine activity handle **70** aiming to increase the bacterial activity selectively for *P. aeruginosa*. The piperidine **70** displays the highest antibacterial activity of the series against *P. aeruginosa* ($\text{MIC} = 107 \pm 12 \mu\text{M}$, Table 3), showing also activity against *E. coli* wild-type K12 ($\text{MIC} = 98 \pm 6 \mu\text{M}$), but suffering simultaneously from efflux (*E. coli* ΔtolC $\text{MIC} = 11 \pm 0 \mu\text{M}$). In comparison, we could determine no MIC for the corresponding primary amine derivative **67** against *P. aeruginosa* wild-type

Table 3. Summary of the biological results of the dichloro-series (compounds 67–70).

				
	67	68	69	70
Enzyme Activity				
EclspE IC ₅₀ (μM)	156 ± 13	36 ± 4	116 ± 14	290 ± 105 μM
PK/LDH IC ₅₀ (μM)	> 500	46 ± 1	> 500	> 500
T _m (°C) [ΔT _m (°C)]	49.60 ± 0.20			
(−1.9)	n.d.	51.31 ± 0.08		
(−0.2)	n.d.			
K _d	~60 μM	n.d.	n.d.	n.d.
Minimum Inhibitory Concentration (MIC) or Percentage Inhibition at 50 μM				
<i>Escherichia coli</i> K12	85 ± 6 μM	58 ± 6% ^[f]	n.i. ^[f]	98 ± 6 μM
<i>Escherichia coli</i> Omp8 ^[b]	45 ± 2 μM	n.d.	n.d.	n.d.
<i>Escherichia coli</i> ΔtolC ^[a]	41 ± 2 μM	2.5 ± 0.1 μM	n.i. ^[f]	11 ± 0 μM
<i>Escherichia coli</i> ΔacrB ^[a]	44 ± 1 μM	n.d.	n.d.	n.d.
<i>Pseudomonas aeruginosa</i>	63 ± 8%	n.d.	n.i. ^[f]	107 ± 12 μM
<i>Acinetobacter baumannii</i>	64 ± 2 μM	n.d.	22 ± 0% ^[f]	32 ± 2 μM
<i>Staphylococcus aureus</i>	99 ± 6 μM	4.8 ± 0.0 μM	33 ± 8% ^[f]	n.d.
<i>Bacillus subtilis</i>	46 ± 1 μM	n.d.	n.d.	n.d.
Cytotoxicity Inhibitory Concentration (IC₅₀)				
HepG2	15 ± 3 μM	33 ± 2 μM	55 ± 3%	7.3 ± 1.7 μM
HEK293	14 ± 1 μM	20 ± 3 μM	49 ± 2 μM	n.d.
Calculated properties				
clogD ^[c]	2.5	5.0	5.6	3.2
Most basic pK _a ^[d]	9.0	N/A	N/A	9.4
Amphiphilic moment ^[e]	4.1	4.1	3.5	6.5

[a] Efflux pump mutant. [b] Porin mutant. [c] Calculated with StarDrop 7.0.1 at pH 7.4. [d] Calculated with StarDrop 7.0.1. [e] Calculated with MOE 2020.09 for the energy-minimised molecule. [f] Experiment performed at 50 μM. n.d.: not determined; N/A: not applicable; n.i.: no inhibition, if inhibition < 10%.

PA14 (%-inh. = 63 ± 8% at 100 μM). Surprisingly, **67** was more active against *E. coli* porin knockdown mutant Omp8 (MIC = 45 ± 2 μM) than against *E. coli* wild-type K12 (MIC = 85 ± 6 μM), which may hint towards porin-independent uptake despite the primary amine. Overall, **67** showed broad-spectrum activity against all tested strains, including the Gram-positive pathogens *S. aureus* and *B. subtilis* (MIC = 99 ± 6 μM and 46 ± 1 μM, respectively, Table 3). The two-fold increase from *S. aureus* to *B. subtilis* can also indicate that the MEP-pathway is a target of **67** although not selectively, as it is utilised by *B. subtilis* but not *S. aureus*. However, cytotoxicity was still a concern and was only reduced in the Boc-derivative **69** with a concomitant loss in antibacterial activity.

Comparison against known antibacterial compounds with similar chemical structure

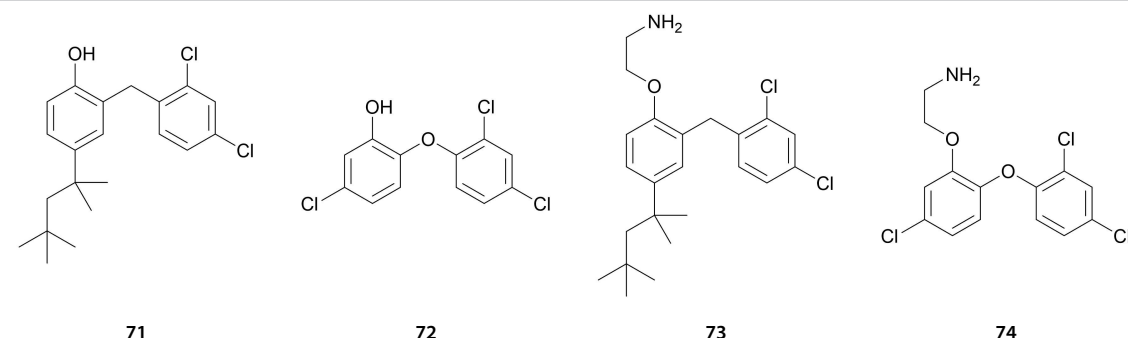
The dichloro-motif, as the 2,4-isomer, is present in two known antibacterial compounds: clofocetol **71** and triclosan **72**. Clofocetol is used against Gram-positive infections of the respiratory tract; it inhibits cell-wall biosynthesis and induces cell-wall permeabilisation, although its exact mechanism of action remains unknown. Currently, **71** is under investigation as a treatment for cancer and SARS-CoV-2.^[24] Triclosan is an additive with disinfectant properties, which interferes with lipid layers at higher concentrations but it also inhibits enoyl-acyl carrier

protein reductase (FabI) at lower concentrations, blocking lipid biosynthesis in susceptible organisms.^[25]

We wanted to see if the introduction of 'our' ethanolamine activity handle (**73** and **74**) could improve their broad-spectrum activity and whether IspE might be their additional target (Table 4). The introduction of the activity handle (Scheme S4) occurred via two-step synthesis and the *N*-Boc intermediates (**75** and **76**) have also been tested (Table S11). In the best case, our

series could dually inhibit two of the key isoprenoid-related biosynthetic pathways, which could be a successful approach to overcome resistance development. The physicochemical properties of clofoctol **71** improved upon introduction of the activity handle (compound **73**) as the amphiphilic moment increased from 6.2 to 8.6 and the clogD value decreased from 7.3 to 4.1 (Table 4). As expected, clofoctol did not inhibit Gram-negative bacteria. Unfortunately, introduction of the activity handle was

Table 4. Summary of the biological results for the known antibiotics clofoctol (**71**) and triclosan (**72**) bearing an ethanolamine activity handle **73–74**.



	71	72	73	74
Enzyme activity				
EclspE IC ₅₀ (μM)	63 ± 11	> 500	97 ± 16	> 500
PK/LDH IC ₅₀ (μM)	22 ± 17	–	137 ± 17	–
Minimum Inhibitory Concentration (MIC) or Percentage Inhibition at 50 μM				
<i>Escherichia coli</i> K12	n.i.	1.3 ± 0.1 μM	32 ± 11 % ^[f]	102 ± 2 μM
<i>Escherichia coli</i> Omp8	34 ± 2 %	n.d.	12.3 ± 2.5 μM	n.d.
<i>Escherichia coli</i> ΔtolC ^[a]	n.i.	0.022 ± 0.000 μM	55 ± 4 % ^[f]	16.7 ± 6.4 μM
<i>Escherichia coli</i> ΔacrB ^[a]	n.i.	0.102 ± 0.040 μM	73 ± 29 μM	48 ± 3 μM
<i>Escherichia coli</i> D22 ^[b]	n.i.	0.20 ± 0.05 μM	n.d.	95 ± 1 μM
<i>Pseudomonas aeruginosa</i>	n.i.	41 ± 5 % ^[f]	n.i.	46 ± 18 % ^[g]
<i>Acinetobacter baumannii</i>	n.i.	4.8 ± 2.0 μM	73 ± 19 %	98 ± 0 μM
<i>Staphylococcus aureus</i>	4.5 ± 1.3 μM	17 ± 11 μM	8.1 ± 2.1 μM	85 ± 1 % ^[g]
<i>Bacillus subtilis</i>	5.4 ± 0.8 μM	5.7 ± 1.2	5.7 ± 0.4 μM	n.d.
Cytotoxicity Inhibitory Concentration (IC₅₀)				
HepG2	12 ± 1 μM	34 ± 10 μM	5.4 ± 0.7 μM	19 ± 3 μM
HEK293	11 ± 2 μM	n.d.	4.3 ± 0.8 μM	n.d.
A549	7.9 ± 1.5 μM	n.d.	9.0 ± 0.4 μM	n.d.
Calculated properties				
clogD ^[c]	7.3	5.0	4.1	2.5
Most basic pK _a ^[d]	N/A	N/A	9.7	8.9
Amphiphilic moment ^[e]	6.2	4.9	8.6	4.9
[a] Efflux pump mutant. [b] Strain with defective LPS layer. [c] Calculated with StarDrop 7.0.1 at pH 7.4. [d] Calculated with StarDrop 7.0.1. [e] Calculated with MOE 2020.09 for the energy-minimized molecule. [f] Experiment performed at 25 μM. [g] Experiment performed at 100 μM. n.d.: not determined. N/A: not applicable. n.i.: no inhibition, if inhibition < 10%.				

only enough to improve clofocetol's antibacterial activity against Gram-negative *E. coli* K12 and *A. baumannii* to 32% and 73% inhibition, respectively. The long aliphatic side chain with increased hydrophobicity might be responsible for the low uptake in Gram-negative pathogens. The Gram-positive activity against *B. subtilis* and *S. aureus* was not affected by the introduction of the activity handle. For the first time, we could measure EclspE inhibitory activity confirming the 2,4-dichloro isomer as an alternative binding motif. Of note, clofocetol's cytotoxicity against HepG2 ($IC_{50} = 12 \pm 1 \mu\text{M}$) is comparable to our series and yet, its further drug-potential is being examined for multiple uses.^[24a]

Attempts to unravel the cytotoxicity issues

With the dichloro-series, we could obtain activity against EclspE and increase the antibacterial activity, but without being able to decrease the cytotoxicity. We also tested mono-halogenated derivatives **54–57** of hit **2** lacking the right-hand side (Table S10). They show no antibacterial activity, confirming the right-hand side is essential for the activity, but also accounts for the cytotoxicity. No toxicity was observed for the chloro-derivative **55** (HepG2 %-inh. = 9 ± 1 at $100 \mu\text{M}$) or iodo-derivative **57** (HepG2 %-inh. = -5 ± 3 at $100 \mu\text{M}$). Therefore, the cytotoxicity seems to stem from the subtle balance between lipophilicity of the aryl core and the basicity of the primary amine, without being influenced by the halogen. This is slightly surprising, as similar diaryl ethers are common building blocks in drug candidates.^[26] To solve the cytotoxicity issues, we next focused on a series using the central phenolic linker whilst changing the activity handle to an aniline derivative due to synthetic accessibility (Table S13, Scheme S5). The best parts including the iodo-motif on the left-hand side of **61** and the dichloro motif on the right-hand side of **68** were combined into **77** (Scheme S5). The compound showed selective EclspE activity ($IC_{50} = 63 \pm 15 \mu\text{M}$, Table S12), a notable increase in binding affinity ($K_D \sim 20 \mu\text{M}$, Table S14) and a clear drop in the melting point ($\Delta T_m = -3.1^\circ\text{C}$, Table S13). It also showed a better antibacterial profile in line with the target profile for inhibiting the MEP pathway (*E. coli* K12 MIC = $47 \pm 2 \mu\text{M}$, *A. baumannii* MIC = $43 \pm 4 \mu\text{M}$, *S. aureus* %-inh. = 87 ± 7 and *B. subtilis* MIC = $30 \pm 10 \mu\text{M}$, Table S12) and no efflux problems, but disappointingly still suffered from a high cytotoxicity against the HepG2 cell line ($IC_{50} = 9 \pm 1 \mu\text{M}$, Table S12), although being comparable to clofocetol (HepG2 $IC_{50} = 12 \pm 1 \mu\text{M}$, Table 3).

Replacing the dichloro-substituents with methyl groups in compound **78** did not alleviate the cytotoxicity (HepG2 $IC_{50} = 12 \pm 1 \mu\text{M}$, Table S12), but the activity against *E. coli* ΔtolC was improved two-fold (*E. coli* K12 MIC = $92 \pm 2 \mu\text{M}$ and *E. coli* ΔtolC MIC = $23 \pm 0 \mu\text{M}$, Table S12). The poorer MIC in *E. coli* K12 suggests the compound being efflux-prone, despite having a low $\text{cLogD} = 1.3$. Using only one chloro-substituent in para-position **79**, maintained the cytotoxicity against HepG2 ($IC_{50} = 28 \pm 6 \mu\text{M}$, Table S12). On the other hand, the replacement of the dichloro substituents by cyano-groups **80** reduced the cytotoxicity two-fold ($IC_{50} = 64 \pm 1 \mu\text{M}$, Table S12), but resulted in a loss of antibacterial activity against *E. coli* K12 ($11 \pm 1\%$ at

$100 \mu\text{M}$, Table S12). Due to the remaining cytotoxicity and lack of EclspE activity, these derivatives were not investigated further.

Instead, we looked into other alternatives to the primary amine and aniline activity handle to **77** (Table 5). Adding a longer aliphatic chain to the aniline **81** or replacing the aniline with a triazole **82** did not alter the antibacterial activity or cytotoxicity profile. Introducing a quaternary amine **83** finally reduced the cytotoxicity without compromising the activity, although the activity against *E. coli* ΔacrB (MIC = $26 \pm 4 \mu\text{M}$) is four-fold lower than that against *E. coli* K12 (MIC = $105 \pm 7 \mu\text{M}$). This suggests that the compound accumulates well in the cytoplasm, but gets recognised for efflux by the *acrB* efflux pump in the inner membrane. As the amphiphilic moment for **83** is low, this result was surprising and indicates that the higher amphiphilic moment may have in fact been driving the cytotoxicity for our series. Unfortunately, none of these derivatives were active against EclspE, which can be partly explained by the predicted binding poses that differ from those of the initial hit **2** (as discussed in detail below). The lack of EclspE engagement is further supported by the increased antibacterial activity against *S. aureus* (MIC = $42 \pm 9 \mu\text{M}$), which is to be expected due to the lack of MEP pathway in *S. aureus*.

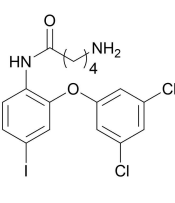
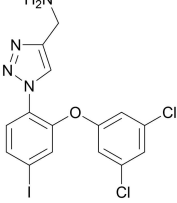
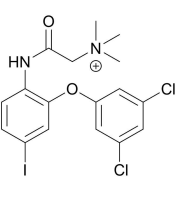
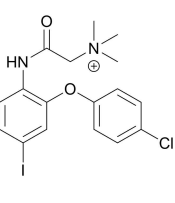
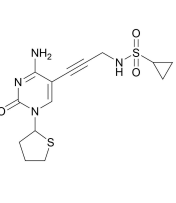
As seen before, removing the dichloro-pattern and replacing it with a *para*-chloro atom instead, lowered cytotoxicity **77** to **79**. The same is true when comparing **83** and **84** (no inhibition of HepG2 of **84**), but *E. coli* K12 activity suffered (MIC = $105 \pm 7 \mu\text{M}$ vs %-inhibition = 36 ± 3).

In summary, we were finally able to mitigate the cytotoxicity by introducing an aniline-activity handle and a *para*-chloro substitution pattern. Compounds **83** and **84** are active against Gram-negative bacteria and show good anti-Gram-positive activity as well. Finding the right balance between lipophilicity, amphiphilic moment and cytotoxicity will remain a challenge for this series of compounds.

Docking analysis to rationalise EclspE activity

Although we found a good starting point to investigate the aniline series further as an antibiotic with no toxicity, in the process, we lost the EclspE activity we were initially looking for. To develop a better understanding of the binding mode of the active compounds, we docked all compounds that we tested against EclspE in vitro to the active site of EclspE in SeeSAR in order to gain insights into why the dichloro-substituents and the primary amine activity handle are necessary for inhibiting EclspE. Interestingly, most compounds that inhibit EclspE have the same, unique binding mode that we saw when introducing the dichloro-substituent (Figure 1). The quality of the ligand–protein interactions represented by the HYDE score given to the compounds by the SeeSAR programme do not correlate with the IC_{50} values but the binding mode is the same for most active compounds (see poses in Table S16). There is always an interaction with His26 via the oxygen atom of the phenolic linker and/or Val156 via the amine of the activity handle. The second phenyl ring with either the dichloro- or no

Table 5. Biological results of derivatives with different activity handles.

					
	81	82	83	84	(±) 92
Enzyme activity					
EclspE IC ₅₀ (μM)	> 500	444 ± 127	> 500	> 500	1.06 ± 0.12
Minimum Inhibitory Concentration (MIC) or Percentage Inhibition at 100 μM					
<i>Escherichia coli</i> K12	91 ± 4 μM	92 ± 2 μM	105 ± 7 μM	36 ± 3 %	n.d.
<i>Escherichia coli</i> ΔtolC ^[a]	43 ± 4 μM	23 ± 0 μM	92 ± 4 μM	46 ± 1 μM	n.i.
<i>Escherichia coli</i> ΔacrB ^[a]	45 ± 2 μM	37 ± 5 μM	26 ± 4 μM	72 ± 11 μM	n.i.
<i>Escherichia coli</i> D22 ^[b]	n.d.	n.d.	72 ± 13 %	49 ± 0 %	n.d.
<i>Pseudomonas aeruginosa</i>	n.d.	n.d.	56 ± 3 %	61 ± 19 %	n.d.
<i>Acinetobacter baumannii</i>	n.d.	n.d.	23 ± 3 %	19 ± 14 %	n.d.
<i>Staphylococcus aureus</i>	n.d.	n.d.	42 ± 9 μM	86 ± 3 %	n.d.
<i>Bacillus subtilis</i>	n.d.	n.d.	23 ± 1 μM	79 ± 17 μM	n.d.
Cytotoxicity Inhibitory Concentration (IC ₅₀)					
HepG2	10 ± 1 μM	15 ± 4 μM	113 ± 36 μM	n.i.	n.i.
HEK293	n.d.	n.d.	81 ± 13 μM	n.d.	n.d.
A549	n.d.	n.d.	94 ± 2 μM	n.i.	n.d.
Calculated properties					
clogD ^[c]	2.6	2.5	2.2	1.8	0.097
Most basic pK _a ^[d]	9.3	9.3	N/A	N/A	6.5
Amphiphilic moment ^[e]	4.9	5.8	3.2	4.6	3.7
[a] Efflux pump mutant. [b] Strain with defective LPS layer [c] Calculated with StarDrop 7.0.1 at pH 7.4. [d] Calculated with StarDrop 7.0.1. [e] Calculated with MOE 2020.09 for the energy-minimized molecule. n.d.: not determined; n.i.: no inhibition, if inhibition < 10%. N/A: not applicable.					

substituents always points in the direction of the Arg72 on top of the adenosine-binding pocket. If the interaction with Val156 is missing, only compounds with a dichlorophenyl group are still active. The activity seems to be dependent on a delicate balance between these three ligand-protein interactions and appropriate substituents since small changes flip the rings, leading to a loss of activity. Especially, the aniline derivatives suffer from this, as the alternative handle does not allow the phenyl rings to orient themselves correctly in the pocket.

Our initial hit compound **2**, although only weakly active (EclspE $K_D \sim 700 \mu\text{M}$), displays the same binding mode while lacking the hydrogen bond to Val156. Other, on first glance inactive, compounds ($\text{IC}_{50} > 500 \mu\text{M}$) display the same binding mode so we assume that they are also weakly binding to IspE. To double check this, we also docked the halogen-series compounds and they all have the correct binding mode (Table S16), but they did not show EclspE inhibition except compound **60**, displaying a decrease in melting point ($\Delta T_m = -1.5^\circ\text{C}$, Table S13).

Compounds that do not follow this trend are **48** and **70**. They are moderately active despite no predicted interaction

with Val156, His26 or Arg22. Instead, they are engaged in an alternative hydrogen bond with Asn12 that we did not observe with any other compound.

Aniline derivative **77** inhibits EclspE ($\text{IC}_{50} = 63 \pm 15 \mu\text{M}$) and binding is also confirmed by MST and TSA although the binding mode suggests no activity. A possible explanation for this is that it is not possible to calculate binding in SeeSAR accurately in all cases, especially since **79** is active, shows the correct binding mode, and only has one chlorine substituent fewer than **77**. The aniline derivatives have to be investigated further and might represent an optimal starting point for further optimisation against EclspE.

These results prompted us to investigate other known IspE inhibitors to compare their proposed binding mode to our compounds. There is one crystal structure published of a compound in complex with *Aquifex aeolicus* IspE (PDB 2VF3) and the close analogue **92** has been previously docked in EclspE with the same binding mode.^[28] Here, we compare sulfonamide **92** with compound **67** that shows all important ligand-protein interactions (Figure 2a–c).

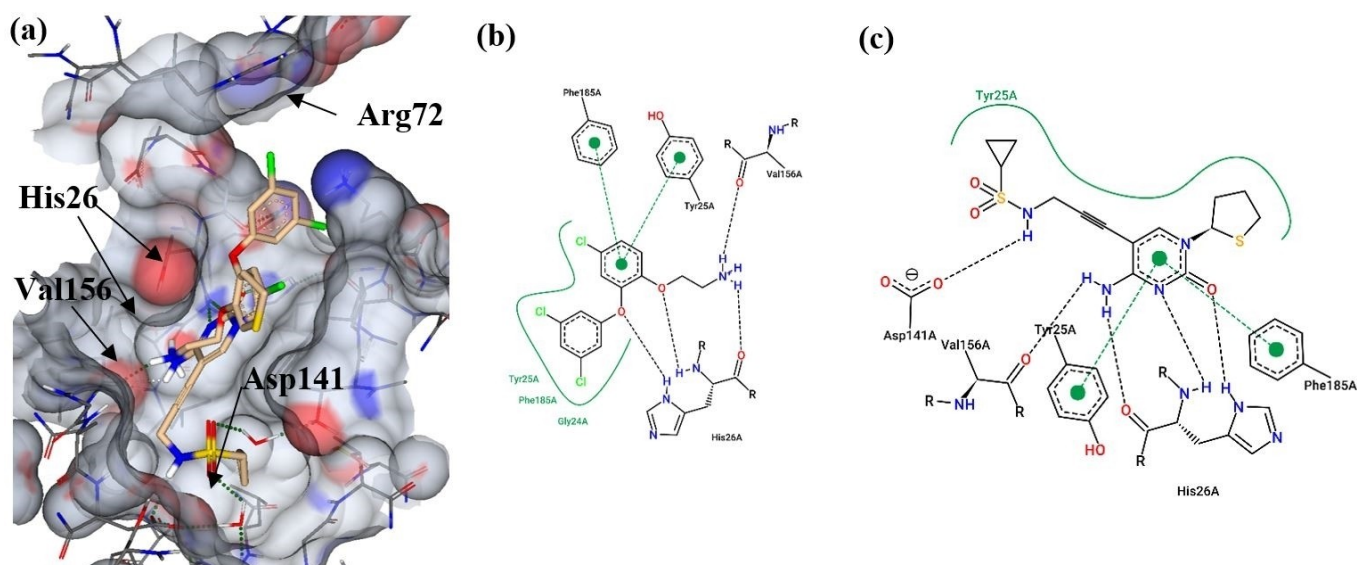


Figure 2. Comparison of docking poses of the LspE inhibitors **67** and **92** in EclspE (PDB 1OJ4). (a) Overlay of both compounds in the binding site of EclspE. Compounds docked in SeeSAR 12.1 and visualized in StarDrop 7.0.1.^[14d] (b) Depiction of binding interactions of compound **67** (c) and previously published sulfonamide **92**. Figures created in Poseview.^[27]

The sulfonamide also forms hydrogenbonds with His26 and Val156. Instead of the hydrophobic interactions with Tyr25, Phe185, Gly24 and the spatial proximity to Arg72, the sulfonamide extends into a hydrophobic region of the pocket and interacts with Asp141.

We envisage a merged compound combining these beneficial interactions will be a potent LspE inhibitor and we will investigate this in the future.

Conclusions

In the search for new LspE inhibitors, we performed a structure-based VS while applying additional rules to improve our chances to find compounds that are active against Gram-negative bacteria. The initial hit **2** suffered from cytotoxicity but showed moderate antibacterial activity and binding to EclspE. Balancing the cytotoxicity, antibacterial activity and enzymatic inhibitory activity turned out to be challenging. Nonetheless, our study resulted in various sub-series with one or the other parameter optimised. Switching from the phenolic core to the aniline series, led by **77**, finally resulted in a new promising direction with the understanding of the drivers for cytotoxicity and antibacterial activity and moreover, EclspE inhibition supported by docking studies. **84** might represent a good starting point for future studies. Although we demonstrate here the challenges associated in bridging the translational gap and finding the ideal balanced profile for this series, we hope these results will support the future discovery of LspE inhibitors as well as the exploration of the chemical space for compound accumulation into bacteria.

Contributions

Conceptualisation, H.-K.R., E.D. and A.K.H.H.; validation, H.-K.R. and S.J.; formal analysis, H.-K.R., S.J., B.I., R.H., J.H. and M.J.; investigation, H.-K.R., E.D, S.J., B.I., R.H., P.S., J.H. and M.J.; resources, M.F. and A.K.H.H.; data curation, H.-K.R., E.D., S.J., B.I., R.H. and J.H.; writing – original draft preparation, H.-K.R., E.D. and S.J.; writing – review and editing, all authors; visualisation, H.-K.R., S.J.; supervision, M.F. and A.K.H.H.; project administration, A.K.H.H.; funding acquisition, H.-K.R. and A.K.H.H. The manuscript stems partly from the doctoral thesis of H.-K.R. (doi:10.22028/D291-34366). H.-K.R. performed her contributions while appointed at HIPS and Saarland University, but is now employed by AMR Action Fund.

Supporting Information

Additional references cited within the Supporting Information.^[29–37]

Acknowledgements

Additional thanks go to J. Herrmann for kindly providing *E. coli* ΔacrB, J.-M. Pagés for kindly providing *E. coli* BL21(DE3)omp8, S. Bousis for the help in establishing TSA and VS, S. Adam for the continuous crystallisation attempts, J. Konstantinović for the help with HRMS measurements, L. Lucaroni for synthesis support, W. A. M. Elgaher for the help with MOE and A. Lacour for support with StarDrop. H.-K.R. thanks the Stiftung Stipendien-Fonds des Verbandes der Chemischen Industrie for the Kekulé Mobility Fellowship. The authors are grateful for the technical support provided by S. Amann, J. Jung, S. Wolter and

D. Jener concerning cytotoxicity and antibacterial assays. Open Access funding enabled and organized by Projekt DEAL.

Conflict of Interests

The authors declare no conflict of interest.

Data Availability Statement

The data that support the findings of this study are available in the supplementary material of this article.

Keywords: MEP pathway · IspE · primary amine · anti-infective · Gram-negative bacteria

- [1] World Health Organization, Antibacterial Agents in Clinical Development: An Analysis of the Antibacterial Clinical Development Pipeline, **2019**.
- [2] H. K. Ropponen, E. Diamanti, A. Siemens, B. Illarionov, J. Hauptenthal, M. Fischer, M. Rottmann, M. Witschel, A. K. H. Hirsch, *RSC Med. Chem.* **2021**, *12*, 593–601.
- [3] A. L. Parkes, *Expert Opin. Drug Discov.* **2020**, *15*, 1005–1013.
- [4] J. Vergalli, I. V. Bodrenko, M. Masi, L. Moynie, S. Acosta-Gutierrez, J. H. Naismith, A. Davin-Regli, M. Ceccarelli, B. van den Berg, M. Winterhalter, J. M. Pages, *Nat. Rev. Microbiol.* **2020**, *18*, 164–176.
- [5] a) M. F. Richter, B. S. Drown, A. P. Riley, A. Garcia, T. Shirai, R. L. Svec, P. J. Hergenrother, *Nature* **2017**, *545*, 299–304; b) M. F. Richter, P. J. Hergenrother, *Ann. N. Y. Acad. Sci.* **2019**, *1435*, 18–38.
- [6] a) Y. Hu, H. Shi, M. Zhou, Q. Ren, W. Zhu, W. Zhang, Z. Zhang, C. Zhou, Y. Liu, X. Ding, H. C. Shen, S. F. Yan, F. Dey, W. Wu, G. Zhai, Z. Zhou, Z. Xu, Y. Ji, H. Lv, T. Jiang, W. Wang, Y. Xu, M. Verccruyse, X. Yao, Y. Mao, X. Yu, K. Bradley, X. Tan, *J. Med. Chem.* **2020**, *63*, 9623–9649; b) B. Liu, R. E. L. Trout, G. H. Chu, D. McGarry, R. W. Jackson, J. C. Hamrick, D. M. Daigle, S. M. Cusick, C. Pozzi, F. De Luca, M. Benvenuti, S. Mangani, J. D. Docquier, W. J. Weiss, D. C. Pevear, L. Xerri, C. J. Burns, *J. Med. Chem.* **2020**, *63*, 2789–2801; c) S. E. Motika, R. J. Ulrich, E. J. Geddes, H. Y. Lee, G. W. Lau, P. J. Hergenrother, *J. Am. Chem. Soc.* **2020**, *142*, 10856–10862; d) E. N. Parker, B. S. Drown, E. J. Geddes, H. Y. Lee, N. Ismail, G. W. Lau, P. J. Hergenrother, *Nat. Microbiol.* **2020**, *5*, 67–75; e) P. A. Smith, M. F. T. Koehler, H. S. Girgis, D. Yan, Y. Chen, Y. Chen, J. J. Crawford, M. R. Durk, R. I. Higuchi, J. Kang, J. Murray, P. Paraselli, S. Park, W. Phung, J. G. Quinn, T. C. Roberts, L. Rouge, J. B. Schwarz, E. Skippington, J. Wai, M. Xu, Z. Yu, H. Zhang, M. W. Tan, C. E. Heise, *Nature* **2018**, *561*, 189–194.
- [7] L. D. Andrews, T. R. Kane, P. Dozzo, C. M. Haglund, D. J. Hilderbrandt, M. S. Linsell, T. Machajewski, G. McEnroe, A. W. Serio, K. B. Wlasichuk, D. B. Neau, S. Pakhomova, G. L. Waldrop, M. Sharp, J. Pogliano, R. T. Cirz, F. Cohen, *J. Med. Chem.* **2019**, *62*, 7489–7505.
- [8] A. Frank, M. Groll, *Chem. Rev.* **2017**, *117*, 5675–5703.
- [9] T. Masini, A. K. Hirsch, *J. Med. Chem.* **2014**, *57*, 9740–9763.
- [10] G. Mombo-Ngoma, J. Rempis, M. Sievers, R. Zoleko Manego, L. Endamne, L. Kabwende, L. Veletzky, T. T. Nguyen, M. Groger, F. Lotsch, J. Mischlinger, L. Flohr, J. Kim, C. Cattaneo, D. Hutchinson, S. Duparc, J. Moehrl, T. P. Velavan, B. Lell, M. Ramharter, A. A. Adegnik, B. Mordmuller, P. G. Kremsner, *Clin. Infect. Dis.* **2018**, *66*, 1823–1830.
- [11] M. S. Davey, J. M. Tyrrell, R. A. Howe, T. R. Walsh, B. Moser, M. A. Toleman, M. Eberl, *Antimicrob. Agents Chemother.* **2011**, *55*, 3635–3636.
- [12] P. Canning, K. Birchall, C. A. Kettleborough, A. Merritt, P. J. Coombs, *Drug Discovery Today* **2020**.
- [13] L. Miallau, M. S. Alphey, L. E. Kemp, G. A. Leonard, S. M. McSweeney, S. Hecht, A. Bacher, W. Eisenreich, F. Rohdich, W. N. Hunter, *Proc. Natl. Acad. Sci. USA* **2003**, *100*, 9173–9178.
- [14] a) A. Volkamer, D. Kuhn, T. Grombacher, F. Rippmann, M. Rarey, *J. Chem. Inf. Model.* **2012**, *52*, 360–372; b) A. Volkamer, D. Kuhn, F. Rippmann, M. Rarey, *Bioinformatics* **2012**, *28*, 2074–2075; c) L. BioSolveIT, **2017**; d) S. BioSolveIT, **2020** and **2022**.
- [15] A. K. Hirsch, M. S. Alphey, S. Lauw, M. Seet, L. Barandun, W. Eisenreich, F. Rohdich, W. N. Hunter, A. Bacher, F. Diederich, *Org. Biomol. Chem.* **2008**, *6*, 2719–2730.
- [16] B. Montefiore, F. Klingler, N. Foster, Poster, **2018**.
- [17] V. Illarionova, J. Kaiser, E. Ostrozhenkova, A. Bacher, M. Fischer, W. Eisenreich, F. Rohdich, *J. Org. Chem.* **2006**, *71*, 8824–8834.
- [18] S. Heuston, M. Begley, C. G. M. Gahan, C. Hill, *Microbiology* **2012**, *158*, 1389–1401.
- [19] A. Prilipov, P. S. Phale, P. Van Gelder, J. P. Rosenbusch, R. Koebnik, *FEMS Microbiol. Lett.* **1998**, *163*, 65–72.
- [20] a) S. Chevalier, E. Bouffartigues, J. Bodilis, O. Maillot, O. Lesouhaitier, M. G. J. Feuilloley, N. Orange, A. Dufour, P. Cornelis, *FEMS Microbiol. Rev.* **2017**, *41*, 698–722; b) A. Dotsch, T. Becker, C. Pommerenke, Z. Magnowska, L. Jansch, S. Haussler, *Antimicrob. Agents Chemother.* **2009**, *53*, 2522–2531; c) L. Fernandez, R. E. Hancock, *Clin. Microbiol. Rev.* **2012**, *25*, 661–681.
- [21] J. Ude, V. Tripathi, J. M. Buyc, S. Soderholm, O. Cunrath, J. Fanous, B. Claudi, A. Egli, C. Schleberger, S. Hiller, D. Bumann, *Proc. Natl. Acad. Sci. USA* **2021**, *118*, 2107644118.
- [22] H. Nikaido, D. G. Thanassi, *Antimicrob. Agents Chemother.* **1993**, *37*, 1393–1399.
- [23] K. B. Hoerchler, **2018**, Graduation thesis
- [24] a) C. Bailly, G. Vergoten, *Drug Discovery Today* **2021**, *26*, 1302–1310; b) F. Yablonsky, *J. Gen. Microbiol.* **1983**, *129*, 1089–1095; c) F. Yablonsky, G. Simonnet, *J. Pharmacol.* **1982**, *13*, 515–524; d) S. Belouzard, A. Machelart, V. Sencio, T. Vausselin, E. Hoffmann, N. Deboosere, Y. Rouille, L. Desmarests, K. Seron, A. Danneels, C. Robil, L. Belloy, C. Moreau, C. Piveteau, A. Biela, A. Vandeputte, S. Heumel, L. Deruyter, J. Dumont, F. Leroux, I. Engelmann, E. K. Alidjinou, D. Hober, P. Brodin, T. Beghin, F. Trottein, B. Deprez, J. Dubuisson, *PLoS Pathog.* **2022**, *18*, e1010498.
- [25] a) R. Khan, A. Zeb, K. Choi, G. Lee, K. W. Lee, S. W. Lee, *Sci. Rep.* **2019**, *9*, 15401; b) P. Shrestha, Y. Zhang, W. J. Chen, T. Y. Wong, *J. Environ. Sci. Health Part C* **2020**, *38*, 245–268.
- [26] T. Chen, H. Xiong, J. F. Yang, X. L. Zhu, R. Y. Qu, G. F. Yang, *J. Agric. Food Chem.* **2020**, *68*, 9839–9877.
- [27] K. Stierand, P. C. Maass, M. Rarey, *Bioinformatics* **2006**, *22*, 1710–1716.
- [28] A. K. Hirsch, S. Lauw, P. Gersbach, W. B. Schweizer, F. Rohdich, W. Eisenreich, A. Bacher, F. Diederich, *ChemMedChem* **2007**, *2*, 806–810.
- [29] C. A. Lipinski, F. Lombardo, B. W. Dominy, P. J. Feeney, *Adv. Drug Delivery Rev.* **2001**, *46*, 3–26.
- [30] J. B. Baell, J. W. M. Nissink, *ACS Chem. Biol.* **2018**, *13*, 36–44.
- [31] R. F. Bruns, I. A. Watson, *J. Med. Chem.* **2012**, *55*, 9763–9772.
- [32] M. O. E. (MOE), Chemical Computing Group ULC, **2018** and **2020**.
- [33] P. Kuzmic, *Anal. Biochem.* **1996**, *237*, 260–273.
- [34] W. A. M. Elgaher, M. Fruth, M. Groh, J. Hauptenthal, R. W. Hartmann, *RSC Adv.* **2014**, *4*, 2177.
- [35] J. Hauptenthal, C. Baehr, S. Zeuzem, A. Piiper, *Int. J. Cancer* **2007**, *121*, 206–210.
- [36] J. M. Peters, A. Colavin, H. Shi, T. L. Czarny, M. H. Larson, S. Wong, J. S. Hawkins, C. H. S. Lu, B. M. Koo, E. Marta, A. L. Shiver, E. H. Whitehead, J. S. Weissman, E. D. Brown, L. S. Qi, K. C. Huang, C. A. Gross, *Cell* **2016**, *165*, 1493–1506.
- [37] S. P. Chavan, P. B. Lasonkar, *Tetrahedron Lett.* **2013**, *54*, 4789–4792.

Manuscript received: July 5, 2023

Revised manuscript received: September 15, 2023

Accepted manuscript online: September 17, 2023

Version of record online: September 28, 2023